# Elastic full waveform Inversion for land walkaway VSP data

*Olga Podgornova, Scott Leaney, Marwan Charara, Schlumberger; Eric von Lunen, Nexen Energy ULC*

## Summary

Full waveform inversion (FWI) is capable of handling multicomponent borehole seismic data and reveals quantitative values of the subsurface medium properties, including compressional and shear-wave velocities. Careful treatment of the source wavelet is crucial for FWI and is a challenging task for land data due to drastic variations of the near-surface conditions. We present a feasibility study of anisotropic elastic FWI for land walkaway vertical seismic profiling (VSP) data acquired in northeast British Columbia, Canada, with a vibrator source. FWI explained the data at medium frequencies and recovered a layered structure of the subsurface that agrees to reasonable accuracy with sonic measurements. The source signature inversion compensated the variation of the near-surface conditions for different offsets.

## Introduction

Vertical seismic profiling (VSP) data are in situ high-frequency and low-noise multicomponent measurements of seismic waves propagating from surface sources to downhole receivers. The numerous borehole seismic events — transmitted, converted and reflected, compressional, shear waves, and multiples — contain rich information on subsurface medium properties. Conventional processing methods of VSP data do not exploit the data up to its limit, although more information may be extracted using advanced processing methods (Campbell *et al.*, 2013). The full waveform inversion (FWI) technique is potentially capable of handling most of the borehole seismic data information and reveals quantitative values of the medium properties, including, but not limited to, compressional and shear-wave velocities.

Applications of FWI to VSP data (Charara *et al.*, 1996; Owusu *et al.*, 2013) confirmed the high expectations of the technique for marine cases. Land data processing is more challenging (for classical processing and imaging methods as well) due to the variability of the near-surface conditions and, as a consequence, the drastic variations of the downgoing wavelets for different source positions. Careful treatment of the source wavelet is crucial for FWI for both marine and land cases, but more practical issues arise for the latter. Several approaches for source wavelet estimation have been discussed in the literature, e.g., Pratt, (1999) in the frequency domain and Rickett (2013) in the time domain, but real data applications for land cases have been limited — e.g., Plessix *et al.* (2012) for acoustic FWI of surface seismic measurements. Here, we present a feasibility study of anisotropic elastic FWI for a land walkaway VSP data set acquired in northeast British Columbia, Canada with a vibroseis source.

## Land VSP data from northeast British Columbia, Canada

Land seismic surveys in northeast British Columbia, Canada, address the goal of delineating the reservoir in the horizontal direction (Campbell *et al.*, 2013). The subsurface geology and topography of the surface are relatively flat. The challenges include rather small compressional reflectivity of the target and the limited illumination of the targeted depths due to high-contrast and high-velocity layers in the overburden. 3D VSP data were acquired by Nexen Energy with a vibroseis source and 135 3C receiver shuttles located from the ground level to 2020 m in depth with a 15-m distance between shuttles. The data were correlated in the field with a 6- to 120-Hz sweep; the data quality of the horizontal components was poor for the deep receivers.

We inverted a two-sided walkaway line, extracted from the 3D data, with 80 shots and with the offsets ranging from 30 m to 2250 m; the shallowest receivers down to 360 m in depth were omitted. Preprocessing includes data rotation to remove the random orientation of the different shuttles, noise reduction, and compensation of the source amplitudes for acquisition effects (Campbell *et al.*, 2013). We use the vertical component and the horizontal component aligned with the walkaway line; the other horizontal component, perpendicular to the walkaway line and ignored in the FWI, has negligible amplitude with the exception of a SH-wave generated at the surface.

## On source wavelet estimation

We use an FWI algorithm with simultaneous inversion of medium parameters and source wavelets. The optimal balance between the source wavelets and model parameters is non-trivial, and alternative approaches for source wavelet estimation are an active research topic (Rickett, 2013). Here, we adjust the weights between the model parameters and the source wavelets empirically (therefore, not in an optimal manner), addressing the feasibility study as the main goal.

We model a vibroseis source as a vertical point force and found that a synthetic SV wave, generated by the source, does not always have a similar counterpart event in the real data. Synthetic simulations confirm that the SV wave is very sensitive to the near-surface medium properties and to the radiation pattern of the source. We let the FWI handle all wave events coming from the overburden (no preprocessing of SV waves) and adjust the shallow part of the model accordingly. FWI was able to retrieve a model of the overburden, explaining fairly well the downgoing wavefields. Whether this model is an equivalent one or it has some geological basis requires further investigation.

## Full waveform inversion algorithm

We apply a conventional least-squares formulation of FWI in the time domain (Tarantola, 1987) with a minimization of the data misfit $\Delta\mathbf{d}(\mathbf{m},\mathbf{q})$ over the model parameters $\mathbf{m}$ and the source wavelet signatures $\mathbf{q}$

$$\Delta\mathbf{d}^T\mathbf{C}_D^{-1}\Delta\mathbf{d}\underset{\mathbf{m},\mathbf{q}}{\rightarrow}\min.$$

We define the source wavelets $\mathbf{q}$ in time separately for each shot and use the weighted norms in the model and the source wavelet spaces with weights $\mathbf{C}_M$ and $\mathbf{C}_Q$, respectively. The matrix $\mathbf{C}_D$ is a covariance matrix in the data space (scalar here). We minimize with a non-linear conjugate gradient algorithm simultaneously for the model and the source wavelets. The gradients are defined as

$$\nabla_m = \mathbf{C}_M\mathbf{G}^\dagger\mathbf{C}_D^{-1}\Delta\mathbf{d}, \quad \nabla_q = \mathbf{C}_Q\mathbf{Q}^\dagger\mathbf{C}_D^{-1}\Delta\mathbf{d},$$

where $\mathbf{G}$ and $\mathbf{Q}$ are the linearized forward modeling operators with respect to the model and source wavelet parameters and $\mathbf{G}^\dagger$ and $\mathbf{Q}^\dagger$ are their adjoints. Basically, the gradient for the model parameters is a crosscorrelation in time of the forward-propagated wavefield and backward-propagated residuals, and the gradient for the source wavelet parameters is the backward-propagated residuals measured at the source location.

We use elastic wave equations in anisotropic VTI media to model the wave propagation and we invert for five parameters: compressional velocity $V_{P0}$, ratio of the compressional and shear velocities $V_{P0}/V_{S0}$, density $\rho$, and Thomsen anisotropic parameters $\varepsilon$, $\delta$ (Thomsen, 1986). We exploit an axial symmetric approximation of the equations (Igel *et al.*, 1996) to reduce the computational cost; this approach is an alternative to a 2D Cartesian algorithm with a data transformation from 3D to 2D space.

We balance the update between the different medium parameters and the values of the source wavelets adjusting the matrices $\mathbf{C}_M$ and $\mathbf{C}_Q$. Additionally, we introduce a spatial correlation in the horizontal and the vertical directions into the matrix $\mathbf{C}_M$ with larger correlation in the horizontal direction to take into account the relatively flat structure of the subsurface.

## FWI strategy and real data results

We started with a layered one-dimensional VTI initial model based on smoothed sonic and density log data and calibrated for anisotropy to fit the traveltimes of the direct P arrivals (Leaney *et al.*, 1999). We filtered the data in the same way for all shots and performed inversion at low frequencies first (up to 25 Hz) and then proceeded with medium frequencies (up to 40 Hz), taking as an initial model the results for low-frequency inversion. The cost function decreases by 70% and 80% for the low and medium frequencies, respectively. The data for small and medium offsets are explained reasonably well, and all major events are reconstructed including the direct wave converted and reflected waves from the major reflectors and some multiples (Figure 1). Distortion of the source wavelet was successfully handled by the source inversion (e.g., Figure 2, A). The misfit was reduced for all source-receiver pairs (Figure 2, B and C) with the exception of several far offsets where the reduction of the misfits was not significant.

FWI updates the initial model and recovers a reasonable layered structure (Figure 3 for $V_{P0}$ and $V_{S0}$). All high-contrast and many small-contrast layers agree with the sonic data with respect to the frequency content of the data used in the inversion. Several small amplitude layers do not fully agree with the sonic data quantitatively and require further analysis.

At this inversion stage, FWI explains most of the transmitted energy and the strong and medium energy reflections. Weaker reflections and medium contrasts at the target depths and above are also identified and can be improved further with a higher-frequency inversion. The model degradation at some distance away from the well (especially visible for the two top high-velocity layers) is the drawback of the current results and is a subject of future work.

## Conclusions

Our feasibility study confirms the robustness of the anisotropic elastic FWI for VSP land data acquired with a vibrator source. Applied to a data set acquired in British Columbia, FWI explained major events in the data at medium frequencies and recovered a layered structure of the subsurface that agrees well with the sonic measurements. The source-signature inversion compensated for the variation of the near-surface conditions for different offsets.

Further improvements include high-frequency FWI to better recover small-amplitude reflections below the high-velocity layers. Analysis of the lateral resolution of the results also remains.

## Acknowledgements

We acknowledge the help and support of Allan Campbell, Les Nutt, Alexsei Shevchenko and Jennifer Leslie-Panek (Nexen). We thank Nexen Energy ULC and Schlumberger for permission.

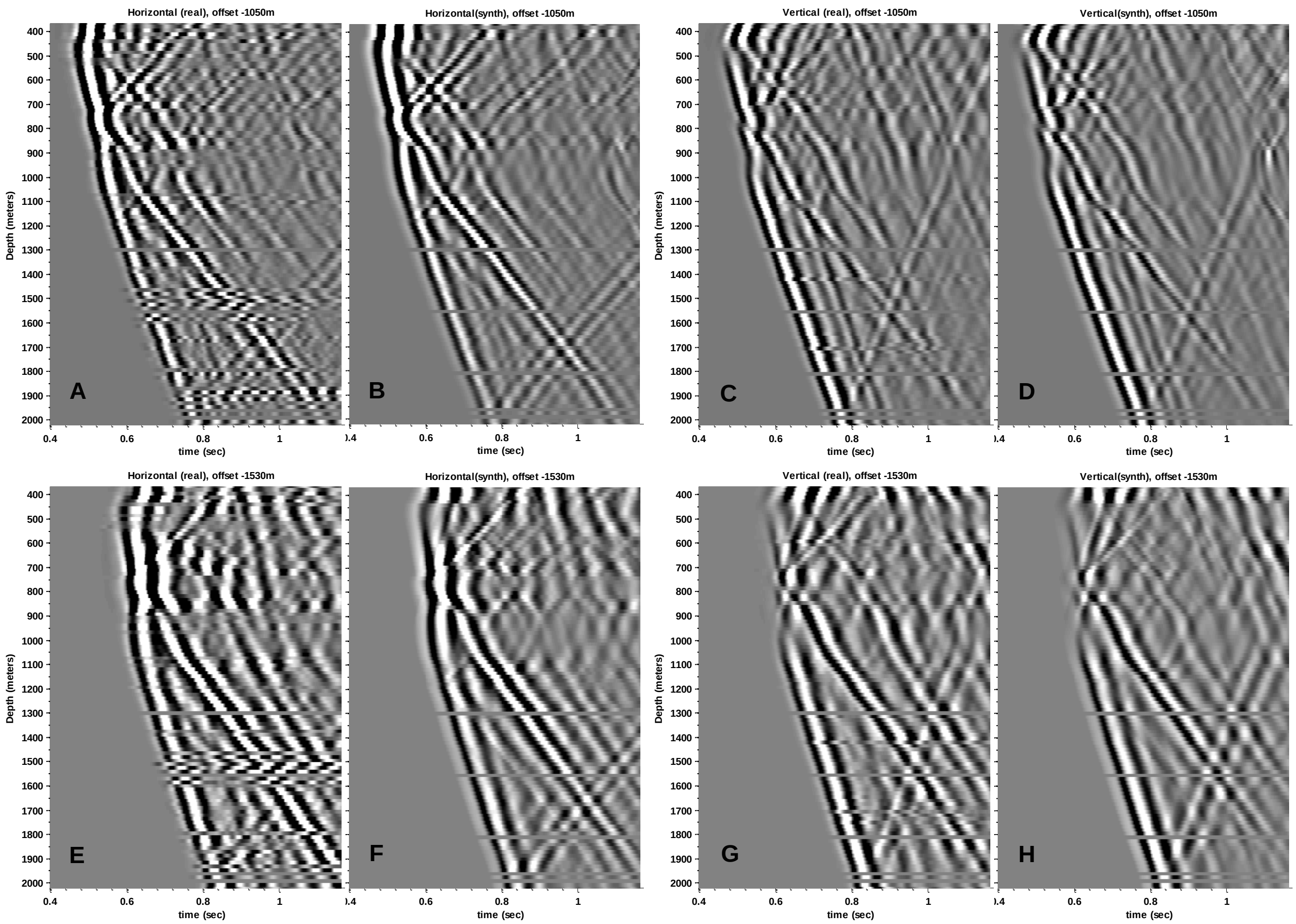


Figure 1: Horizontal and vertical components of real (A, C) and synthetic (B, D) data for an offset ~1050 m filtered up to 40 Hz. Horizontal and vertical components of real (E, G) and synthetic (F, H) data for an offset ~1530 m. Frequency filtering of the real data is the same for all offsets. Several receivers were corrupted or switched off (blank and noisy traces).

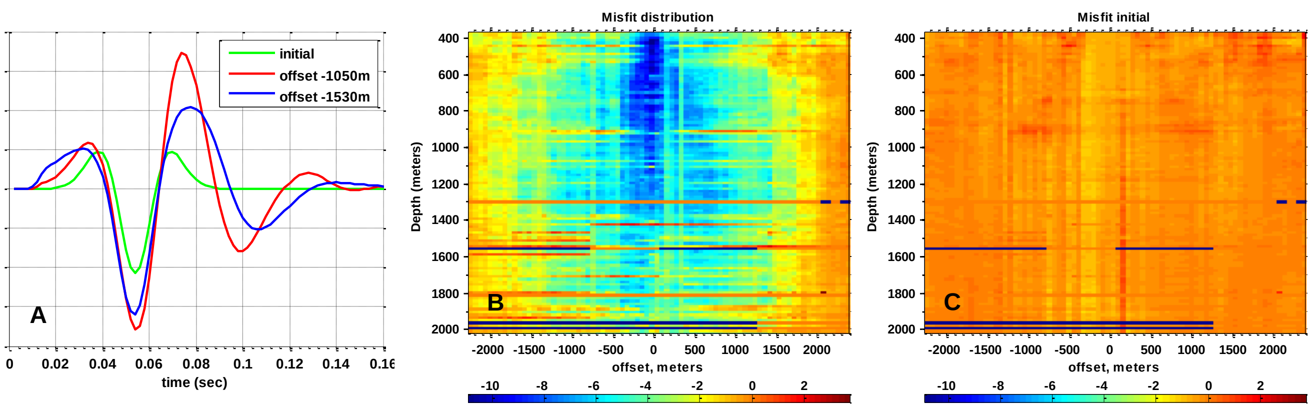


Figure 2: Inverted source wavelets for two offsets, the same as in Figure 1 (A). Final (B) and initial (C) distributions of the misfit between all source receiver pairs in logarithmic scale for medium frequencies; each shot is scaled separately.

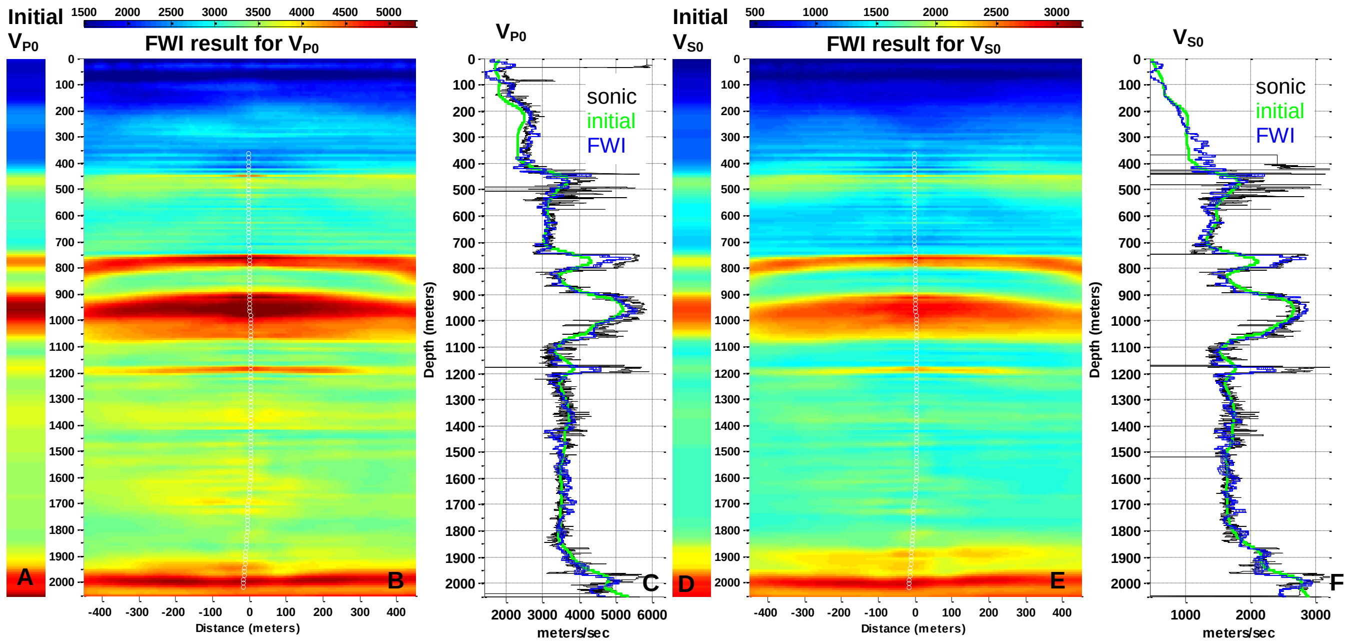


Figure 3: Initial 1D model (A) and FWI result (B) for $V_{P0}$. Sonic data, initial model, and FWI result in the vicinity of the well for $V_{P0}$ (C). The same goes for $V_{S0}$ (D, E, F). White circles (in B and D) correspond to the receivers positions.

## References


Campbell, A., Leaney, S., Gulati, J., Leslie-Panek, J., and Von Lunen, E., 2013, Images, anisotropy, multiples, and more from an unconventional 3D VSP: The Leading Edge, **32**(10), 1238-1244.

Charara, M., Barnes, C. and Tarantola, A., 1996, The state of affairs in inversion of seismic data: an OVSP example. 66th Annual International Meeting, SEG, Expanded Abstracts, 1999–2002.

Igel, H., Djikpéssé, H. and Tarantola, A., 1996, Waveform inversion of marine reflection seismograms for P impedance and Poisson's ratio: Geophysical Journal International, **124** (2), 363–371.

Leaney, S., Cao, D. and Tcherkashnev, S., 1999, Calibrating anisotropic, anelastic models for converted-wave simulation: 61st EAGE Conference & Exhibition, Extended Abstracts, 6–52.

Owusu, J.C., Podgornova, O., Charara, M., Leaney, S., Campbell, A., Ali, S., Borodin, I., Nutt, L. and Menkiti, H., 2013, Anisotropic Elastic Full-waveform Inversion for a Real Walkaway VSP Data from The Arabian Gulf – Towards High Frequencies: 75th EAGE Conference & Exhibition, Extended Abstracts.

Plessix, R.E, Baeten, G., de Maag, J., ten Kroode, F. and Rujie, Z., 2012, Full waveform inversion and distance separated simultaneous sweeping: a study with a land seismic data set: Geophysical Prospecting, **60**, 733–747.

Pratt, R.G., 1999, Seismic waveform inversion in the frequency domain, Part I: Geophysics, **64**, 888–901.

Rickett, J., 2013, The variable projection method for waveform inversion with an unknown source function. Geophysical Prospecting, **61**, 1365-2478.

Tarantola, A., 1987, Inverse problem theory, methods for data fitting and model parameter estimation: Elsevier.

Thomsen, L. A., 1986, Weak elastic anisotropy: Geophysics, **51**, 1954–1966.